Geotechnical Engineering in the XXI Century: Lessons learned and future challenges
N.P. López-Acosta et al. (Eds.)

doi:10.3233/STAL190073

Experimental and Numerical Evaluation of the Effect of Compaction-Induced Stress on Reinforced Soil Walls Performance

S. H. MIRMORADI[a,1] and M. EHRLICH[a]
[a]*Federal University of Rio de Janeiro, UFRJ, RJ 21945-970, Brazil*

Abstract. The influence of the compaction-induced stress is experimentally and numerically evaluated on the behavior of reinforced soil walls (RSWs), under working stress conditions. Experimental studies have been carried out to evaluate the effect of the compaction condition at the back of the block facing on the behavior of geosynthetic-reinforced soil walls. Three large-scale geosynthetic-reinforced soil walls were constructed at the COPPE/UFRJ Geotechnical Laboratory. The walls were well-instrumented to monitor the values of the reinforcement load, toe horizontal load, horizontal facing displacement, horizontal stress on the back of the block facing, and vertical displacement at the top of the walls. The numerical analyses have been carried out using the 2D finite element program Plaxis considering two different procedures for modeling of the compaction-induced stress found in the literature. The numerical analyses were validated using data from a full-scale well-instrumented geosynthetic-reinforced soil wall. The results of the experimental studies and numerical analyses are presented and discussed.

Keywords. Compaction-induced stress, reinforced soil walls, experimental study, numerical analysis.

1. Introduction

The effect of backfill compaction on the behavior of reinforced soil (RS) walls has been investigated and discussed in some studies found in the literature [e.g. 1-6]. The results, in general, showed that the induced stress due to backfill compaction may represent a kind of pre-stressing of RS walls and may reduce lateral displacement after wall construction.

Some recommendations have been made regarding the compaction conditions of the backfill near the facing such as using lightweight compaction equipment (recommended by the Federal Highway Administration) [7] or placing higher quality backfill in this zone to obtain the desired properties with reduced compaction effort in order to minimize the compaction-induced outward deformation and lateral stresses against the back of the facing. In the experimental section of the paper three large-scale geosynthetic-reinforced soil (GRS) walls, were analyzed to understand the importance of the compaction condition near the back of block facing.

[1] Corresponding Author; E-mail: shm@ufrj.br.

Numerical modelling may be a powerful tool to properly represent field conditions, if boundary conditions, geometry, constitutive models, parameters, and representative modelling procedure are correctly employed. Regarding the numerical simulation of the compaction-induced stress (CIS), it is important to know which procedure may better represent the actual field condition. In the numerical section of the paper, two numerical procedures found in the literature for modelling of the CIS are presented and the results of the numerical analyses are compared with the measured values from the laboratory experiment.

2. Experimental study

2.1. Test characteristics and material used

Instrument data and measurements from three physical model walls constructed at the Geotechnical Laboratory of COPPE/UFRJ are used to evaluate the effect of compaction near facing on the behavior of GRS walls under working stress conditions [8]. These walls are herein identified as Wall 1, Wall 2, and Wall 3. Figure 1 shows a cross-section of a physical model. The walls were constructed in a U-shape concrete box that is 1.5 m high, 3.0 m long, and 2.0 m wide. The height of the wall was 1.2 m. Three layers of polyester geogrid were installed at 0.2 m, 0.6 m, and 1.0 m from the wall bottom. The vertical spacing of reinforcements and the facing inclination were 0.4 m and 6° to the vertical, respectively. Precast concrete block was used for the face of the walls.

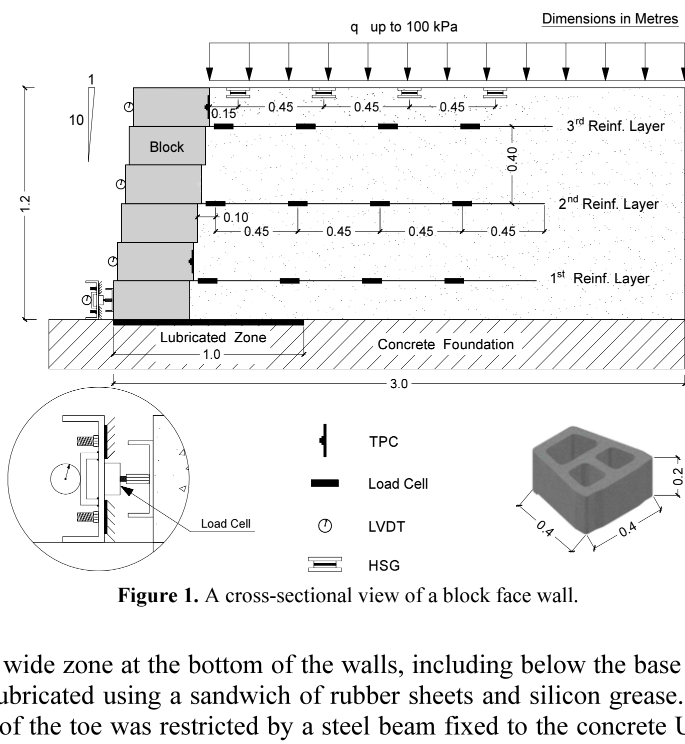

Figure 1. A cross-sectional view of a block face wall.

A 1-m wide zone at the bottom of the walls, including below the base of the block face, was lubricated using a sandwich of rubber sheets and silicon grease. The lateral movement of the toe was restricted by a steel beam fixed to the concrete U-shape wall box as shown in Figure 1. At the end of construction of the walls, a vertical surcharge up to 100 kPa was applied on top of the walls. The surcharge was then kept constant on 100 kPa and the toe of the wall was released step by step (0.5 mm horizontal movement allowed in each step) to reach to the free base condition [9, 10].

In Wall 1, the entire surface of the backfill layers was compacted using a light vibrating plate (8 kPa; hereafter referred to as the "light compactor"). In Wall 2, first the entire surface of the backfill layers was compacted using a light compactor, and then the backfill, except for 0.5 m from the back of the facing, was compacted using a vibratory tamper (63 kPa; hereafter referred to as the "heavy compactor"). For Wall 3, the entire surface of the backfill layers was compacted first by light compactor and subsequently using the heavy compactor.

The soil unit weights after light and heavy compactions were 19 and 20 kN/m^3, respectively. The soil friction angles, considering the measured unit weight, were determined by triaxial and plane strain compression tests as 42°and 50°, respectively. The walls were instrumented to monitor the values of the reinforcement load, horizontal toe load, horizontal facing displacement, horizontal stress on the back of the block facing, and vertical displacement at the top of the walls. Additional information about properties of the backfill soil and instrumentation could be found in [8, 11, 12].

2.2. Test results

Figure 2 shows the sum of the maximum reinforcement loads, T_{max}, at the end of construction (EOC), during surcharge application and toe release. The figure indicates that although the values of T_{max} are different at the EOC, this difference decreases as the applied surcharge increases and at the end of loading (EOL) similar values were measured for all walls irrespective of the compaction conditions that agrees with the discussion presented by [1, 4]. They stated that compaction of backfill using heavy compaction equipment may lead to a significant increase in the reinforcement load and this increase may vanish when the surcharge value exceeds the corresponding value of the vertical stress induced by heavy compaction. Figure 2(b) also illustrates that ΣT_{max} increases for the walls during toe release. Nevertheless, this increase is greater for the walls in which the backfills were compacted using light and heavy compactor equipment (i.e., Wall 2).

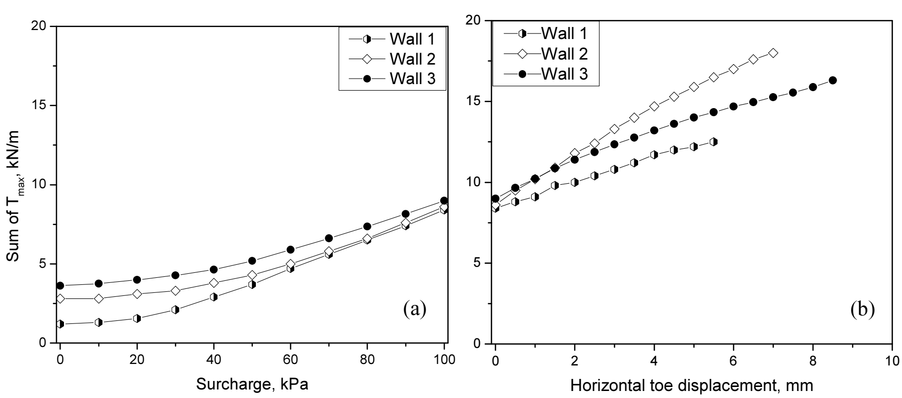

Figure 2. Sum of maximum reinforcement load (a) during surcharge application and (b) toe release.

Figure 3 illustrates the measured values of the horizontal displacements during construction (Figure 3a) and the average of the post-construction horizontal displacements (H_{ave}) versus surcharge application (Figure 3b). The figure shows that in Wall 3, in which the entire surface of the backfill was compacted using the vibratory tamper, the highest and lowest horizontal facing displacement occur during construction and post-construction, respectively. This is an expected behavior as the heavy compaction promotes displacement during the construction period and reduces post-construction horizontal displacement. This means that heavy compaction may cause the reinforced soil mass to exhibit a kind of over-consolidation that promotes a stiffer behavior after construction [1, 4]. Nevertheless, this behavior is not observed for Wall 2.

Furthermore, Figure 3 indicates that both during construction and the post-construction horizontal displacement in Wall 2 are higher than that in Wall 1. This is also observed in Figure 4, in which the vertical displacement measured using hydraulic settlement gage (HSG) at four positions at the end of loading and toe release are presented. The figure shows the significantly greater vertical displacements for Wall 2 in the first (0.15 cm from the back of the face) and second measurement positions (0.6 cm from the back of the face) compared with Walls 1 and 3. On the other hand, in the third (105 cm from the back of the face) and fourth measurement positions (150 cm from the back of the face), similar values were obtained for all walls. It is also indicated that the lowest vertical displacement values were measured in Wall 3 [8].

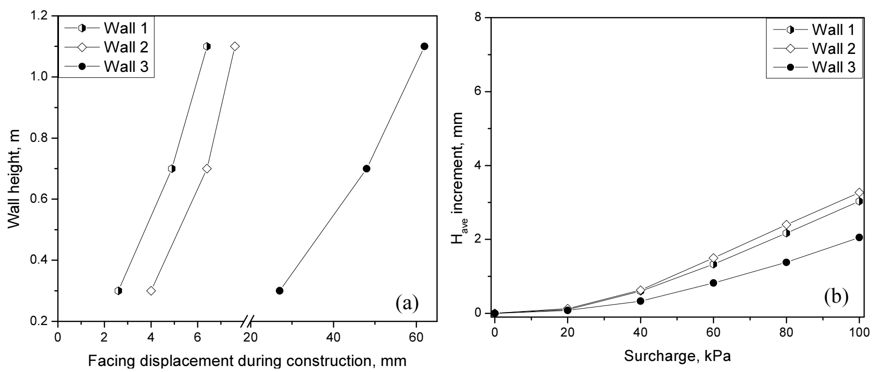

Figure 3. Horizontal facing displacement (a) during construction and (b) post construction.

As stated earlier, in Wall 2, the backfill was firstly compacted with the light compactor. Then the heavy compactor was used except for the first 0.5 m of backfill directly behind the facing. The high vertical displacement of the backfill located close to the back of the facing may be associated with an increase of the void ratio of the soil near to the face due to the vibration promoted by the operation of the tamper equipment nearby. This can be clearly seen in Figure 4, in which, the backfill soil unit weights versus distance from the facing is presented for the walls. As shown, in Walls 1 and 3, the average backfill unit weights of 19 and 20 kN/m^3 were measured after the end of compaction operations, irrespective of the distance from back of facing. In Wall 2 however, the magnitude of the soil unit weight measured in the first 0.5 m zone was lower than (~5%) those measured in Wall 1, in which the same compactor equipment (light compactor) was employed in the entire surface of the soil layers. This highlights the importance of the compaction condition close to the back of the facing [8].

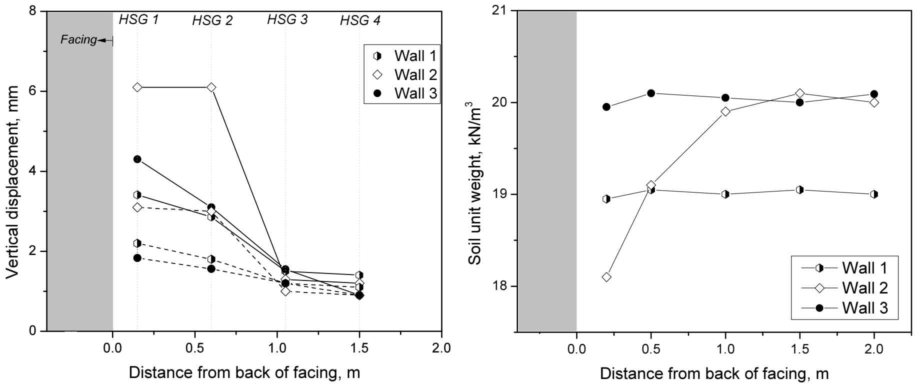

Figure 4. Vertical displacement at the end of surcharge application, EOL (dashed lines), and toe release, EOR (solid lines) and backfill soil unit weight for three walls.

3. Numerical study

3.1. Model characteristics

Numerical modeling was performed for block-face MSE walls using the 2D finite element program PLAXIS [13]. Data from a full-scale reinforced soil wall built at the Royal Military College of Canada (RMC) was used to validate the numerical modeling for a block-face wall [14].

The wall was 3.6 m high, with a facing inclination of 8° to the vertical. The length and vertical spacing of the geogrid were 2.52 m and 0.6 m, respectively. Reinforcement was modelled as a linear elastic material with perfect interface adherence to the adjacent soil. The input parameters were the same as those used by [15]. Details about the model can be found in [16, 17].

The wall was constructed in stages; i.e. 0.15 m thick soil lifts were placed and compacted until the final wall height was reached. Two different methods were employed for modelling the compaction-induced stress as follows:

I) Applying a uniform vertical stress to the top of each backfill soil layer as the wall was being modelled from the bottom up, as suggested in the literature [e.g., 14] (referred to as procedure type I).

II) Applying a distribution load at the top and bottom of each soil layer, as suggested by [16] (referred to as procedure type II).

Regarding the compaction condition of the physical model considered in this study, it should be mentioned that the first 0.5 m directly behind the wall-facing was hand-tamped to a target 95% of standard Proctor density, using a rigid steel plate to minimise construction-induced outward deformation and lateral stresses against the back of the facing. The backfill located beyond 0.5 m of the facing was compacted in 150 mm lifts using three passes of a walk-behind, gasoline-powered, vibrating-plate compactor (Whacker VPG-155A) with a dynamic contact pressure of 55 kPa [3]. For the numerical modelling of compaction, the vertical stress of 8 kPa was used to model the CIS in the first 0.5 m behind the facing, and the value of 55 kPa was employed for the backfill located beyond 0.5 m of the facing [17].

Figure 5 shows two different approaches for the simulation of the induced stress due to compaction. Figure 5a and b shows a schematic view of the numerical modelling of compaction-induced stress using a distributed load, q_c, at the top of each soil layer (type I); and distribution loads, q_c, at the top and bottom of each soil layer (type II), respectively. Four steps for backfill soil construction in a specific soil layer, n, were considered: (I) soil layer placement, (II) compaction equipment operation, (III) end of compaction, and (IV) next soil layer placement (layer n+1). Figure 5a, step (II) shows that when procedure type I is used for numerical modelling of the induced stresses due to compaction in soil layer n, it leads to a constant increase in the vertical stress due to compaction, q_c, in all layers below. The dashed line in this figure shows the expected vertical stress increased during the roller operation for soil layer n based on the strip load elastic solution, where its maximum value takes place at soil-roller contact and decreases significantly with depth. This figure clearly shows that using the distribution load solely at the top of each soil layer when modelling compaction cannot match the actual field conditions represented by the elastic solution [17].

Figure 5b shows a schematic view of procedure type II, as suggested by [11, 16] for the numerical simulation of the induced stress due to compaction. Figure 5b, step (II) shows that when procedure type II is used for the soil layer n, all points in this soil layer would be driven to the same vertical stress increase. In addition, for the soil layers placed under this layer, only geostatic stresses occur. A comparison between the curves related to the compaction modelling using procedure type II, and the dashed line represented by the elastic solution, indicates that this procedure may be more representative of the actual induced vertical stress during roller operation [17].

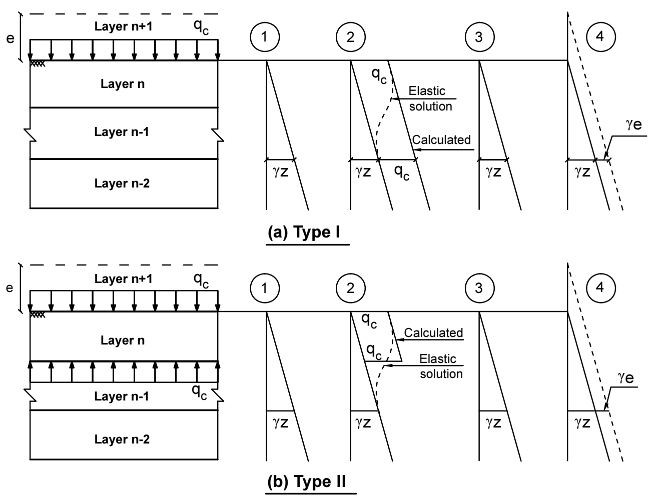

Figure 5. Modelling of the vertical stress load–unload cycles verified during the compaction of the backfill layer, using compaction procedures types I and II.

3.2. Results of analyses

Figure 6a shows a comparison between the calculated and measured values of the horizontally-facing displacement at the end of construction. A comparison between the measurements and the values calculated by PLAXIS using compaction procedure type I show that this modelling setup leads to significantly greater facing displacement values.

The results show that the measured values of the facing displacement were reasonably well predicted by PLAXIS when compaction procedures type II was employed [17].

Figure 6b shows that the measured values of the connection loads were reasonably well predicted by PLAXIS when compaction procedure type II was employed, except for in the first two layers near the bottom of the wall. However, the connection load values calculated by PLAXIS for the model using compaction procedure type I was significantly higher than those measured [17].

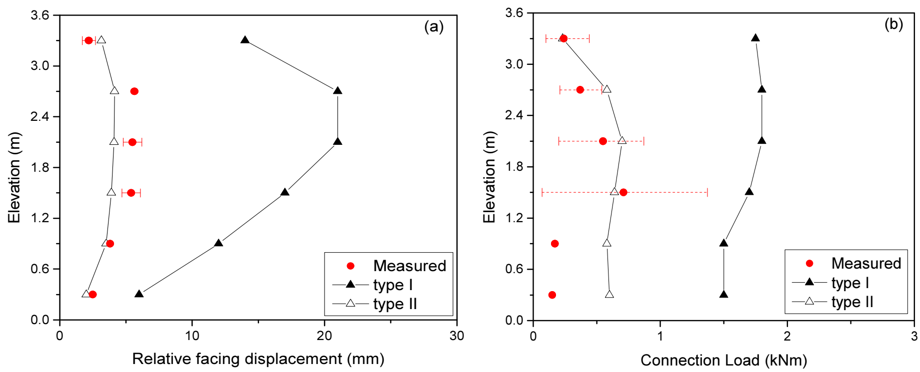

Figure 6. Measured and calculated values of the a) horizontally-facing displacement at the end of construction and b) connection load.

4. Conclusions

Experimental and numerical studies have been carried out to evaluate the effect of the compaction induced stress on the behavior of GRS walls. Three large-scale GRS walls with different compaction condition at the back of block facing were constructed at the COPPE/UFRJ Geotechnical Laboratory to evaluate the effect of this factor on the wall performance. The numerical analyses were carried out considering two different procedures to simulate the compaction-induced stress, CIS and the results of the modelling were compared against the data from a full-scale GRS segmental wall built at the Royal Military College of Canada RMC.

The results of the experimental study highlight the importance of the compaction conditions close to the back of the facing. It is shown that when the backfill near the back of block facing is not adequately compacted, the maximum reinforcement loads, horizontal and vertical displacements of the GRS wall increase during construction and post construction. It should be noted that in the real fieldwork, on one hand, it is common to prevent operation of heavy compactors behind the facing to minimize compaction-induced outward deformation and lateral stresses against the back of the facing. On the other hand, due to inadequate compaction in this zone, the wall may present unexpected behavior as observed in the performed tests. Therefore, it may be a good specification for backfill compaction to be compacted using tamper compaction in the interval of 0.5–1.0m behind the facing and roller compaction beyond that. Tamper compaction may lead to a more similar compaction induced stress found in a typical roller compaction [5, 8].

Considering the compaction modelling by applying a uniform vertical stress to the top of each backfill layer, the numerical analyses significantly overestimate the measured values of the reinforcement strains, connection loads and facing displacement. When the compaction was simulated by applying a distribution load at the top and bottom of each soil layer satisfactory agreement has been generally observed between measurements and calculated values.

Acknowledgments

The authors greatly appreciate the funding of this study by the Brazilian Research Council, CNPq, and the Brazilian Federal Agency for Support and Evaluation of Graduate Education, CAPES. We also thank Flavio Montez and Andre Estevao Ferreira da Silva from the Huesker Company for their support, as well as Cid Almeida Dieguez for his support in performing the experiments.

References

[1] Ehrlich, M., Mitchell, J.K., Working stress design method for reinforced soil walls, J. Geotech. Eng. ASCE 120 (4), (1994), 625-645.
[2] Tatsuoka, F., Uchimura, T., Tateyama, M., Preloaded and pre-stressed reinforced soil, Soils Found. 37 (3), (1997), 79-94.
[3] Bathurst, R.J., Nernheim, A., Walters, D.L., Allen, T.M., Burgess, P., Saunders, D.D., Influence of reinforcement stiffness and compaction on the performance of four geosynthetic reinforced soil walls, Geosynth. Int. 16 (1), (2009), 43-59.
[4] Ehrlich, M., Mirmoradi, S.H., Saramago, R.P., Evaluation of the effect of compaction on the behavior of geosynthetic-reinforced soil walls, J. Geotextile Geomembr. 34, (2012), 108-115.
[5] Ehrlich, M., Mirmoradi, S.H., A simplified working stress design method for reinforced soil walls, Géotechnique, 66 (10), (2016), 854-863.
[6] Mirmoradi, S.H., Ehrlich, M., Numerical Evaluation of the Behavior of GRS Walls with Segmental Block Facing under Working Stress Conditions, ASCE J. Geotech. Geoenviron. Eng., 141 (3), (2015b), 04014109.
[7] Berg, R., Christopher, B.R., Samtani, N., Mechanically Stabilized Earth Walls and Reinforced Soil Slopes, Design and Construction Guidelines, U. S. Department of Transportation, Federal Highway Administration, Washington, DC, p. 668. FHWA-NH1-09-083 and FHWA GEC011, 2009.
[8] Mirmoradi, S.H., Ehrlich, M., Experimental evaluation of the effect of compaction near facing on the behavior of GRS walls, J. Geotextile Geomembr., 46(5), (2018a), 566-574.
[9] Mirmoradi, S.H., Ehrlich, M., Evaluation of the Effect of Toe Restraint on GRS Walls, Transportation Geotechnics, SI: Geosynthetics in Tpt, 8, (2016), 35-44.
[10] Mirmoradi, S. H., Ehrlich, M., and Dieguez, C., Evaluation of the Combined Effect of Toe Resistance and Facing Inclination on the Behavior of GRS Walls, J. Geotextile Geomembr., 44(3), (2016) 287-294.
[11] Ehrlich, M., Mirmoradi, S.H., Evaluation of the effects of facing stiffness and toe resistance on the behavior of GRS walls, J. Geotextile Geomembr., 40 (Oct), (2013), 28-36.
[12] Mirmoradi, S.H., Ehrlich, M., Geosynthetic Reinforced Soil Walls: Experimental and Numerical Evaluation of the Combined Effects of Facing Stiffness and Toe Resistance on Performance, Proc., 10th Int. Conf. on Geosynthetics, International Society of Soil Mechanics and Geotechnical Engineering (ISSMGE), London, 2014.
[13] Brinkgreve, R. B. J., and Vermeer, P. A. PLAXIS: Finite element code for soil and rock analyses, version 8, CRC Press/Balkema, Leiden, Netherlands, 2002.
[14] Hatami, K., Bathurst, R.J., Development and verification of a numerical model for the analysis of geosynthetic reinforced-soil segmental walls, Can. Geotech. J. 42 (4), (2005), 1066-1085.
[15] Guler, E., Hamderi, M., Demirkan, M.M., Numerical analysis of reinforced soil retaining wall structures with cohesive and granular backfills, Geosynth. Int. 14 (6), (2007), 330-345.
[16] Mirmoradi, S.H., Ehrlich, M., Modeling of the Compaction-induced Stress on Reinforced Soil Walls, J. Geotextile Geomembr., 43 (1), (2015a), 82-88.
[17] Mirmoradi, S.H., Ehrlich, M., Numerical simulation of compaction-induced stress for the analysis of RS walls under working conditions, J. Geotextile Geomembr., 46, (3),(2018b), 354-365.